

Atomic-level characterization of liquid/solid interface

Jiani Hong(洪嘉妮), Ying Jiang(江颖)

Citation:.Chin. Phys. B . 2020, 29(11): 116803 . **doi:** 10.1088/1674-1056/aba9d0
Journal homepage: http://cpb.iphy.ac.cn; http://iopscience.iop.org/cpb

What follows is a list of articles you may be interested in

Atomic-level characterization of liquid/solid interface

Jiani Hong(洪嘉妮), Ying Jiang(江颖)
Chin. Phys. B . 2020, 29(11): 116803 . **doi:** 10.1088/1674-1056/aba9d0

Epitaxial growth of antimony nanofilms on HOPG and thermal desorption to control the film thickness

Shuya Xing(邢淑雅), Le Lei(雷乐), Haoyu Dong(董皓宇), Jianfeng Guo(郭剑峰), Feiyue Cao(曹飞跃), Shangzhi Gu(顾尚志), Sabir Hussain, Fei Pang(庞斐), Wei Ji(季威), Rui Xu(许瑞), Zhihai Cheng(程志海)
Chin. Phys. B . 2020, 29(9): 096801 . **doi:** 10.1088/1674-1056/aba27c

Analysis of meniscus beneath metastable droplets and wetting transition on micro/nano textured surfaces

Yanjie Li(李艳杰), Xiangqin Li(李香琴), Tianqing Liu(刘天庆), Weiguo Song(宋伟国)
Chin. Phys. B . 2018, 27(8): 086801 . **doi:** 10.1088/1674-1056/27/8/086801

Interfacial nanobubbles produced by long-time preserved cold water

Li-Min Zhou(周利民), Shuo Wang(王硕), Jie Qiu(邱杰), Lei Wang(王磊), Xing-Ya Wang(王兴亚), Bin Li(李宾), Li-Juan Zhang(张立娟), Jun Hu(胡钧)
Chin. Phys. B . 2017, 26(10): 106803 . **doi:** 10.1088/1674-1056/26/10/106803

Vibrational features of confined water in nanoporous TiO_2 by Raman spectra

Xin Gao(高欣), Qiang Wang(王强), Gang Sun(孙刚), Chen-Xi Li(李晨曦), Lin Hu(胡林)
Chin. Phys. B . 2016, 25(2): 026801 . **doi:** 10.1088/1674-1056/25/2/026801

TOPICAL REVIEW — Water at molecular level

Atomic-level characterization of liquid/solid interface

Jiani Hong(洪嘉妮)[1] and Ying Jiang(江颖)[1,2,3,†]

[1] International Center for Quantum Materials, School of Physics, Peking University, Beijing 100871, China
[2] Collaborative Innovation Center of Quantum Matter, Beijing 100871, China
[3] CAS Center for Excellence in Topological Quantum Computation, University of Chinese Academy of Sciences, Beijing 100190, China

(Received 8 May 2020; revised manuscript received 6 July 2020; accepted manuscript online 28 July 2020)

The detailed understanding of various underlying processes at liquid/solid interfaces requires the development of interface-sensitive and high-resolution experimental techniques with atomic precision. In this perspective, we review the recent advances in studying the liquid/solid interfaces at atomic level by electrochemical scanning tunneling microscope (EC-STM), non-contact atomic force microscopy (NC-AFM), and surface-sensitive vibrational spectroscopies. Different from the ultrahigh vacuum and cryogenic experiments, these techniques are all operated *in situ* under ambient condition, making the measurements close to the native state of the liquid/solid interface. In the end, we present some perspectives on emerging techniques, which can defeat the limitation of existing imaging and spectroscopic methods in the characterization of liquid/solid interfaces.

Keywords: liquid/solid interface, atomic scale, scanning tunneling microscope (STM), atomic force microscopy (AFM)

PACS: 68.08.–p, 68.37.–d, 68.37.Ef, 68.37.Ps **DOI:** 10.1088/1674-1056/aba9d0

1. Introduction

Liquid/solid interfaces are ubiquitous in nature and play essential roles in a broad spectrum of fields ranging from chemical and physical processes to biological science.[1–3] Due to the reason that what we are interested in is buried at the interface between two bulk phases, a complete atomic-level understanding is extremely challenging. Such buried interfaces are not directly accessible to conventional surface-sensitive spectroscopic techniques except for a few cases under some restrictions.[4–7] In addition, most of the high-resolution imaging methods require extreme conditions of ultrahigh vacuum and cryogenic temperature, which are not compatible with the liquid environment. Therefore, *in situ* studies of the liquid/solid interfaces from an atomic-scale perspective are extremely difficult.

A promising new tool to overcome this difficulty is liquid-phase scanning probe microscope (SPM), which permits high-resolution measurements under ambient conditions. The liquid-compatible microscopy is applicable for characterizing liquid/solid interfaces straightforwardly.[8] As an important member of SPM family, scanning tunneling microscope (STM) can achieve real-space visualization of surfaces at atomic scale.[9,10] Based on this, electrochemical STM (EC-STM) has been developed to understand the underlying microscopic mechanisms of electrochemical reactions by monitoring single molecules or even atoms at the solid-electrolyte interfaces, not only *in situ* but also *in operando*.[11,12] The information obtained by EC-STM can shed new lights onto various electrochemical phenomena, including adsorptions relevant to the formation of electrochemical double layer,[13,14] catalysts,[15,16] corrosion,[17,18] deposition,[19,20] and so on. However, the interpretation of EC-STM images is usually complicated by the electronic structure of the sample and the EC-STM experiments are limited to conducting surfaces.

Non-contact atomic force microscopy (NC-AFM) shows the ability to overcome the aforementioned limitations, which can achieve atomic images of both solutes and solvents near the insulating surfaces because of its high sensitivity to the short range forces and local liquid density.[21] With the advantages noted above, two-dimensional (2D) and three-dimensional (3D) mapping experiments at liquid/solid interfaces have been conducted by NC-AFM on a wide variety of substrates broadly existing in nature, such as minerals,[22] organic films,[23] and biomolecules.[24,25] Local hydration structures on surfaces can also be identified by NC-AFM, which may help to establish the atomic-level understanding of various interfacial processes in solution.[26]

Despite the outstanding performance of SPM, the measurements are susceptible to the perturbance of the dynamic molecules in the liquid induced by tunneling current or interaction forces. Moreover, the SPM lacks the chemical information. In contrast, interface-sensitive and non-invasive vibrational spectroscopies have proven to be useful tools to acquire molecular-level information both structurally and chemically.[27] Nevertheless, it is well known that those techniques suffer from the broadening and averaging effects due

†Corresponding author. E-mail: yjiang@pku.edu.cn

© 2020 Chinese Physical Society and IOP Publishing Ltd

to the poor spatial resolution. This bottleneck can be relieved with the help of theoretical calculations to some extent.[28]

In this perspective, we place emphasis on scanning probes techniques applied in the atomic-scale investigation of liquid/solid interface, since spectroscopic techniques have been discussed briefly on this subject in the previous reviews.[29–31] The article is organized as following. In Section 2, we begin with a review of advances in EC-STM for probing adsorbates, metal deposition, catalysis, corrosion, etc. After that, we introduce the applications of NC-AFM and its 3D imaging mode, paying special attention to interfacial hydration layers. Next, we overview the interfacial studies by vibrational spectroscopies with a focus on water–solid interaction. The potential and newly developed techniques for high-resolution characterization of liquid/solid interfaces are envisaged in Section 3, in terms of SPM based on nitrogen-vacancy center, multifunctional AFM for battery characterization, *ex-situ* SPM measurements, and cryo-STEM. Finally, a summary is delivered.

2. Existing techniques in liquid/solid interface studies

2.1. Electrochemical scanning tunneling microscope

As a powerful tool for providing atomic imaging of liquid/solid interface not only *in situ* but also *in operando*, EC-STM can help us obtain unique insights into electrochemical processes. Compared with traditional STM, EC-STM has four electrodes (tip, working electrode, counter electrode, and reference electrode) controlled by bipotentiostate in the system, which allows imaging at the defined potential even when the potential of the working electrode is changing.[11] What is more, the majority of tip in EC-STM is coated with insulating layers except for the top end of it, in order to minimize the interference induced by Faraday currents within the tunneling gap (Fig. 1(a)).[32,33]

The potential of the charged metal electrode is screened by the solvated ions in the solution, forming the so-called electrochemical double layer (EBL).[34] EBL plays a significant role in electrochemical reaction, and the atomic-scale structural information is also very important. Adsorption of ordered anions within the EBL region on the low-index metal electrode surfaces has been studied extensively.[13,35] As weakly solvated ions, halide anions can partially lose their hydration shell leading to strong interaction with substrate and form ordered structures on it. Such structures show a universal phenomenon of halide anion-induced reconstruction[36,37] and a distinct potential-dependent phase behavior[38,39] with not only commensurate structures but also incommensurate structures due to the competing adsorbate–adsorbate and adsorbate–substrate interactions. The interfacial electrochemistry of sulfide anions is more intricate and shows more phases than the halide anions.[40,41] Taking the copper substrate as an example, on Cu (111) surface, no reconstruction is induced by the adsorbates and the phases at different potentials can reversibly transform into each other by creating or annihilating defects with the exchange of the sulfur atoms with the near-surface solution layer.[42] While on Cu (100) surface, sulfide adsorbates can induce reconstruction with an expansion of Cu–Cu interatomic distance by 9% on the first layer of electrode when the potential sweeps positively.[43] Moreover, although termed as pseudo-halide, thiocyanate anions behave more like a pseudo-chalcogenide in high consistency with the behavior of sulfide.[44] It should be noted that anions in solution may affect the process of metal dissolution, which is regarded as an aspect of corrosion science by stabilizing[35,45] or disordering[46,47] the step orientation with a high metal mobility.[48] The anions can combine with cations into complexes, leading to high mobility at the surface,[37] that is to say, inducing etching of metal surface via a step flowing mechanism.

Adsorption of cations in relevance to the process of electrodeposition depends decisively on the morphology of the electrode[49,50] and the given potential corresponding to different coverage stage of the deposited metal.[51] Underpotential deposition (UPD) and overpotential deposition (OPD) are two phenomena distinguished by the Nernst potential in the process of a cathodic potential scanning. It was found that the anions pre-occupy on surface. For example, the bisulfate and chloride can compete with metal adatom for surface sites or even impede the UPD process.[50,52,53] While in some cases, metal atoms tend to combine with anions to form a bilayer for their lattice match with substrate, such as the Cd layer sandwiched between a Cl overlayer and the first layer of the Cu(111) substrate, generated by exchanging between the pre-adsorbed Cl anions and adsorbing Cd cations.[54] Similar CuCl structure was also found on Pt(111) surface.[55] Relating to the growth of metal multi-layers, overpotential deposition of metal can be characterized by EC-STM as well, exhibiting co-adsorption of metal layers and anion species.[56]

The liquid/solid interface offers a proper platform to investigate self-assembled molecular systems. Structure and the properties of self-assembled molecular monolayers absorbed on flat substrates can be revealed by STM on the nanoscale, which indicates that the long-range ordering is dictated by the interplay between the molecule–molecule interactions and molecule–substrate interactions. Apart from coordinate covalent bonds,[57] noncovalent interactions such as hydrogen bonding interactions,[58–60] halogen bonding interactions,[61–64] and van der Waals (vdW) interactions,[65–67] are commonly emerged as intermolecular interactions. Moreover, temperature,[68–70] concentration as well as solvent[71,72] can also affect the self-assembly behav-

ior. Self-assembly of organic molecules at the sold–liquid interface investigated by STM has been summarized in many excellent review articles.[73–76]

Additional electrochemical environments offered by EC-STM opened the possibility of controlling surface dynamics and structures via surface charge.[77,78] The structures of adsorbed molecules are modified with pre-absorbed anions and their phase transition is determined not only by the change of electrode potential but also by redox-induced change of charge state of molecules themselves.[79–86] Notably, some observations show that the adsorption of water molecules lowers the work function of metal surface[87] and water molecules can be identified in general at the interface by EC-STM,[88,89] serving to screen the electrostatic repulsions between the absorbed anions. However, the detailed molecular characteristics of water on electrochemical interfaces have remained poorly understood due to the reason that the tip could easily disturb the water molecules or other delicate metastable structures, which is still a tough problem calling for new technical breakthroughs.

Apart from the atomic characterization of electrochemical interfacial layer as described above, EC-STM also provides a new way to address heterogeneous catalysis.[90,91] Recently, catalytically active surface sites can be identified directly at atomic scale under reaction condition by EC-STM. The key lies in monitoring time-varying current noise, which results from the temporal tunneling barrier fluctuations induced by local redox reaction (Figs. 1(b) and 1(c)). It was discovered that only one to three Pd atoms located at Au/Pb boundaries contributed greatly to the hydrogen-evolution reaction activity (Figs. 1(d) and 1(e)).[92–94] Furthermore, a well-known phenomenon that metal surface can undergo a concomitant transformation[95] during the oxidation-reduction cycles (ORC) in electrolyte was investigated by EC-STM likewise.[96] There are two roughing processes on Pt(111) surface, namely, "nucleation and early growth" and "late growth". With the number of ORC increasing, both of the two processes contribute to the roughening of the electrode, while every step site created in the latter contributes equally to the electrochemical signal. A detailed atomistic picture was derived by Leon *et al.*[97]

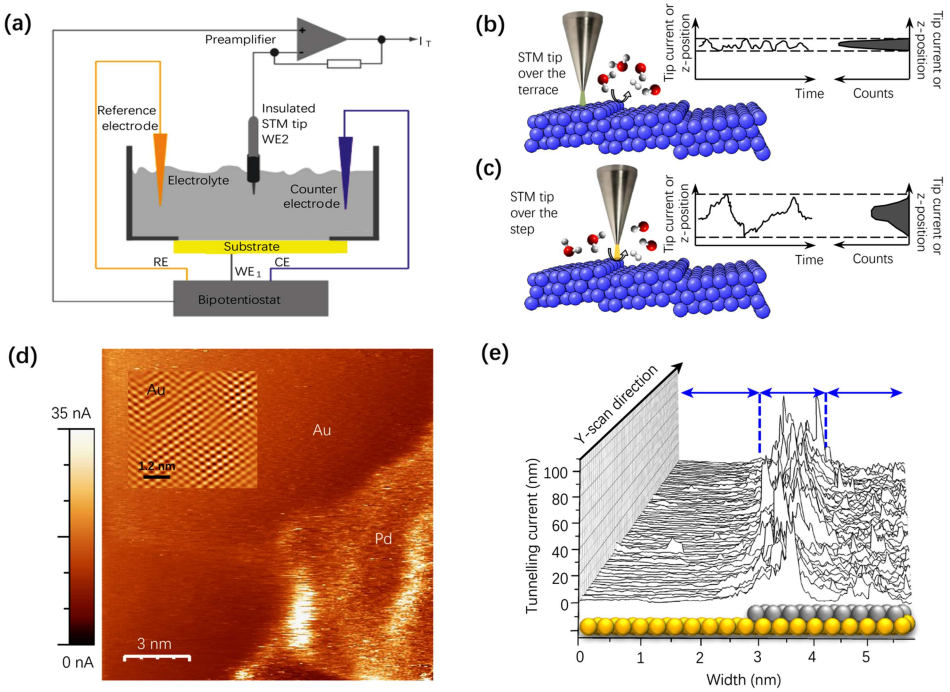


Fig. 1. (a) The configuration of EC-STM, where the bipotentiostat controls the potential of the substrate (WE_1), STM tip (WE_2), and counter electrode (CE) with respect to the reference electrode (RE). The majority of STM tip is coated with insulation. (b)–(c) Schematic diagram of the concept of detecting catalytic sites. The tunnelling barrier varies with the change of local environment between the STM tip and sample, arising from the attachment and detachment of reactants and products. Tunnelling-current noise is larger in the case of scanning over a step shown in (c) than that over a terrace in (b), suggesting that step sites are more active than terrace steps, and the noise is reflected on the z-position when STM is operated in constant-current mode. (d) Constant-height STM image of the boundary between a Pd island and Au (111) substrate under hydrogen evolution reaction (HER) conditions in 0.1 M sulfuric acid. (e) Detailed tunnelling-current line scans for the boundary shown in (d). Panels (b)–(e) reproduced with permission from Ref. [92].

2.2. Non-contact atomic force microscopy

Another indispensable tool for characterizing liquid/solid interfaces is NC-AFM, which is able to monitor and analyze the multiple interfacial interactions on both conductive and insulating substrates with atomic resolution.[98] NC-AFM often operates dynamically with the cantilever excited near its resonance frequency. Amplitude, frequency as well as phase shift of cantilever are three measurable quantities. According to different detected signals used for feedback control, NC-AFM can further be classified into amplitude modulated

AFM (AM-AFM) and frequency modulated (FM-AFM).[99] Both of the two operational modes have been applied in ultrahigh vacuum (UHV) environments to achieve ultrahigh spatial resolution.[100–102] However, visualizing atomic-scale structures at a liquid/solid interface is very challenging, due to the low Q factor of the cantilever resonance in liquid[103] and the large thermal drift at ambient temperature.[104] Those problems have been tackled by developing low-noise cantilever deflection sensor[105] and various drift-compensated data acquisition schemes,[106,107] making atomic resolution possible even in liquids.

Since the first atomic-resolution topographic images were obtained by FM-AFM with a low-noise cantilever deflection sensor at mica–water interface,[108] this technique has been used extensively for various samples, ranging from inorganic crystals, such as $SrTiO_3$,[109] TiO_2,[110] calcite,[111–113] clay and aluminosilicate minerals,[114] to interfacial organic molecules, polyethylene films immersed in n-dodecane[115] and polypropylene films in a buffer solution,[116] various liquid hydrocarbons facing alkanethiol monolayers,[117] thiolate monolayer,[118] etc. What is more, it is also viable in imaging biomolecules, for example, lipid bilayers,[119,120] proteins,[121,122] lysozyme,[123] self-assembled antibodies,[124] and DNA molecules.[125] Recently, topographic images of rutile TiO_2 in aqueous KCl solution with various pH values were acquired by Xue *et al.*, revealing a transition of protuberate structure from (1×1) meshes in acidic or neutral solutions to $P(2 \times 1)$ superstructure in alkaline solutions due to the chemisorption of OH^- species on five-fold coordinated Ti cations.[126] Based on this technique, Miyata *et al.* developed high-speed FM-AFM at 1 s/frame and revealed an intermediate $Ca(OH)_2$ layer along the step edge in calcite dissolution process.[127]

Apart from the low-noise detection mode by soft and small silicon cantilevers ($k \approx 0.1$–10 N/m, $f_0 > 100$ kHz), a stiffer q-Plus sensor ($k \geq 1$ kN/m)[128] maintaining a much higher Q than the Si cantilever in liquid is emerged as a powerful tool for high signal-to-noise (SNR) interfacial study, such as biologically-relevant environments[129] or more viscous ionic liquid interface.[130–132] Compared with the soft silicon cantilever which uses optical methods to detect its deflection, the q-Plus sensor is self-sensing by utilizing the piezoelectricity of quartz, making it suitable for imaging in non-transparent solutions. Moreover, q-Plus sensor allows simultaneous acquisition of the tunneling current and the tip–sample interaction forces. Nevertheless, q-Plus sensor is much stiffer than silicon cantilevers and its higher stiffness k and lower center frequency f_0 can result in a lower force sensitivity and a greater detector noise. In order to obtain high SNR images, the scanning speed of the q-Plus sensor should be slowed down since the detector noise is also proportional to the bandwidth. Therefore, the image capture rate in the case of q-Plus senor is smaller than that of cantilever.[129]

The force between tip and sample can be measured in a three-dimensional (3D) way. The first measurement of 3D force fields was done on NiO(111) surface in vacuum.[133] As a spectacular extension of NC-AFM, 3D-AFM can even provide detailed atomic-scale insights on liquid/solid interface not only laterally but also vertically, which opens the door to understand distance-dependent behaviors of the interactions between the surface and interfacial solvent or solute.[26,134] There are two common protocols for high-quality 3D data acquisition to eliminate or reduce the large thermal drift during the long-time acquisition of massive data for building up the 3D images: the "curve-by-curve approach"[135] and "layer-by-layer" approach.[136]

The existence of stable hydration layers has been verified by NC-AFM in 2D case,[137] triggering subsequent investigation of hydration layers on various surfaces to clarify the central role they play in a wide range of chemical phenomena and biological processes.[138] Visualization of hydration layers in the direction vertical to surface was achieved by 3D-AFM for the first time on muscovite mica.[122,139,140] By combining bimodal AFM operation[141] with 3D-AFM, Å resolution with high scanning speed (sub-minute) was obtained by Herruzo *et al.*[142] at mica–water interface subsequently. The dependence of interfacial structures on the concentration and type of electrolyte was observed at mica–electrolyte interface.[143] It was revealed that the cations tended to form monolayer on mica covered by only several hydration layers at low salt concentration (Figs. 2(a) and 2(b)). For higher concentration, the interfacial layers became thicker (Figs. 2(d)–2(f)) with the lateral periodicity close to that of the substrate (Fig. 2(c)), while the vertical periodicity was determined by the interactions between the ions and the water molecules.

Surface structures of carbonates in aqueous are vital in numerous areas due to their importance in a range of fields, such as biomineralization and geochemistry.[144,145] As prototypical kinds of carbonates, calcite, dolomite as well as magnesite were studied widely by 3D-AFM[146–148] and atomistic simulation.[149,150] In all cases mentioned above, three hydration layers and checkerboard pattern were observed on carbonate–water interface and resembled an epitaxial growth commensurate to the underlying crystal lattice. Besides, chemical identification between Ca and Mg cations could be achieved through the subtle difference in their hydration structures at the dolomite–water interface.[151]

The 3D-force mapping has been applied not only to inorganic substrates, such as mica and carbonates mentioned above, α-Al_2O_3,[152] graphite,[153] but also to organic molecular interfacial layers[117,118,154] and molecular crystals.[155] Furthermore, this technique can be even extended to biological

systems for understanding the interfacial biological processes with molecular detail.[117,137,156] Interfacial behaviors of liquid 1-decanol were studied on graphite, showing four liquid layers above the physicosorbed decanol columns that are epitaxial to the substrate.[157] Lateral heterogeneity in the first and second layers may be induced by competition between hydrogen bonding and van der Waals interactions because of slightly different stacking situations of decano.

In addition to measurements on atomically flat homogeneous mineral surfaces aforementioned, Umeda *et al.* succeeded in visualizing atomic-scale interfacial 3D hydration on a heterogeneously charged phyllosilicate surface (Fig. 3). Combined with molecular dynamics simulations, they found that the lateral water distribution was in accordance with the local lattice periodicity and no clear hydration structures were observed at the boundary between the two surface regions with opposite charges, arising from the ion depletion due to the neutral step edge effect.[158]

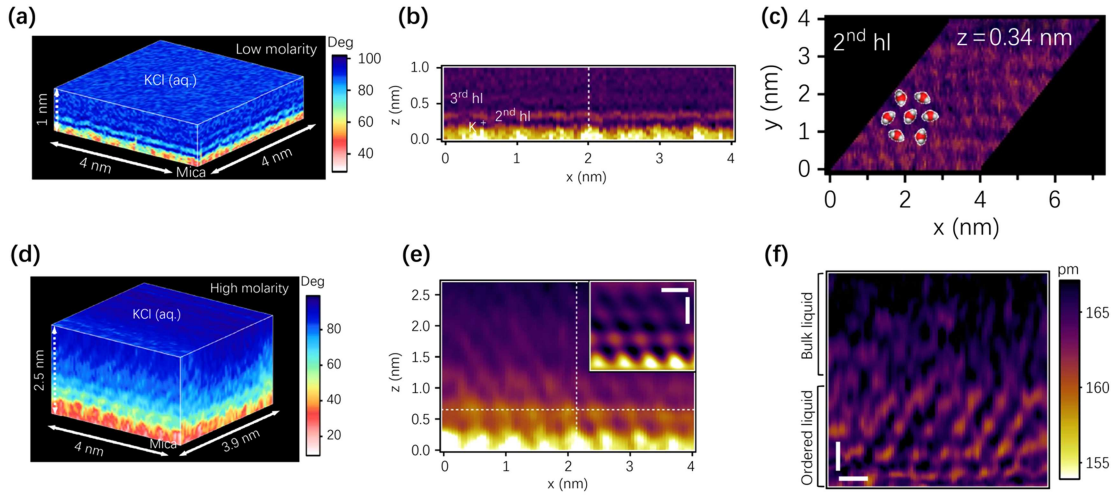


Fig. 2. (a) 3D AFM image of aqueous KCl/mica interface in the case of low molarity (0.2 M KCl). A monolayer of K^+ (red color) is absorbed on mica topped by two hydration layers (0.3 nm thick), which follow the corrugation of substrate (lighter stripes). (b) *XZ* frame of (a) (raw data). The ordered layer at interface is very thin (below 1.0 nm). (c) *XY* frame taken at $z = 0.34$ nm. The structure of the water molecules in the 2nd hydration layer is revealed. The origin of z is chosen at the mica surface (minima in (b)). (d) 3D AFM image of aqueous KCl/mica interface for high molarity (4 M KCl). Interfacial layers can be divided into two regions, ordered liquid layers (2 nm thick) and bulk liquid above it. (e) *XZ* frame of (d) (low pass filtered image). An ordered liquid layer extending up to 2–3 nm from the mica at high molarities is characterized at the interface. The inset shows a filtered image (FFT) of the bottom right corner of the *XZ* frame. (f) *XZ* frame extending 5 nm above the mica surface. Reproduced with permission from Ref. [143].

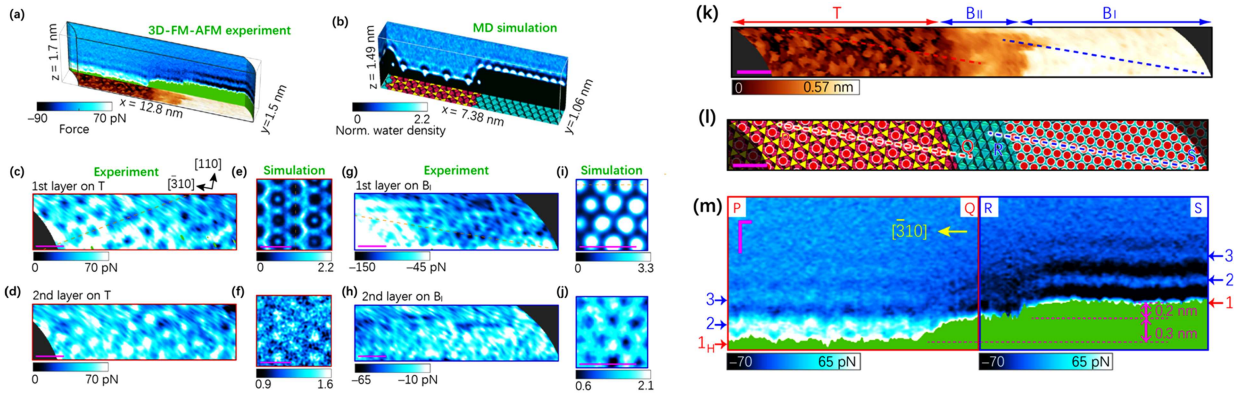


Fig. 3. (a)–(b) 3D FM-AFM image and MD simulation on the water/clinochlore (001) interface across an area including the T, B_{II}, and B_I regions shown in (k), respectively. (c)–(f) Experimental lateral 2D force maps and theoretical lateral 2D-normalized water (oxygen) density maps of 1st and 2nd layers on T region, respectively. Honeycomb-like pattern of the first hydration layer and a dot-like pattern of the second hydration layer were observed both in AFM experiments and simulations. (g)–(l) Lateral 2D force maps and theoretical lateral 2D-normalized water (oxygen) density maps of 1st and 2nd layer on B_I region, respectively. Atomic-scale patterns of both layers observed in experiments and simulations show the same lattice constant. (k)–(l) Topographic image and structural model around the step edge, respectively. Adsorbed water molecules are represented as red dots in (l). (m) *XZ* force maps along the broken lines P–Q and R–S in (l). Reproduced with permission from Ref. [158].

2.3. Surface-sensitive vibrational spectroscopies

One shortage of SPM is the susceptibility to the perturbance of the dynamic molecules in the liquid induced by tunneling current or interaction forces. Moreover, chemical information cannot be easily obtained by SPM. Surface-sensitive vibrational spectroscopies have been proven to be well suited for molecular-level characterization of the surface and interfacial processes in solution, including sum frequency gener-

ation (SFG) vibrational spectroscopy, surface-enhanced Raman spectroscopy (SERS), tip-enhanced Raman spectroscopy (TERS), and so on. Those methods are almost non-invasive to the liquid/solid interfacial structure and provide valuable chemical identity through vibrational fingerprints.

SFG gains the high sensitivity to explore liquid/solid interface since its signals are only generated from non-centrosymmetric media,[159,160] involving interfacial biological systems,[161,162] absorbed organic molecules,[163,164] electrochemical systems,[165,166] interfacial ionic liquids,[167,168] etc. The interaction of water molecules with solid substrates has been a key issue in the field of SFG, which could be obtained through the O–H stretching signals.[169–172] It was found that the water structure underwent order–disorder–order change with the change of pH and the orientation of water molecule could flip by 180° when the pH of the aqueous solution crossed the isoelectric point of the quartz surface.[169] What is more, Yang *et al.* associated the suppressed ordering of water structures at small pH with poor ice nucleation on mica coated by sulfuric acid.[173]

The dependences of interfacial water structure on electrode potential[174] and cations in solution[175–178] were also widely investigated at molecular scale. It should be mentioned that among these studies, SFG signals originate from two regions at the charged water interface, labeled as "the bonded interface layer (BIL)", which is ordered and closest to the surface, and "the diffuse layer (DL)", which is next to BIL in bulk H-bonding structure and can be affected by the surface field (Fig. 4(a)). Therefore, the interpretation of the vibrational spectra is very tricky and the subtle details of water–solid interaction can be easily smeared out. In 2016, Wen *et al.* separated the spectral information of these two regimes successfully at lipid–aqueous interface and revealed different microscopic structures of water molecules in BIL, arising from various charge states of the lipid headgroup (Figs. 4(b)–4(d)).[179]

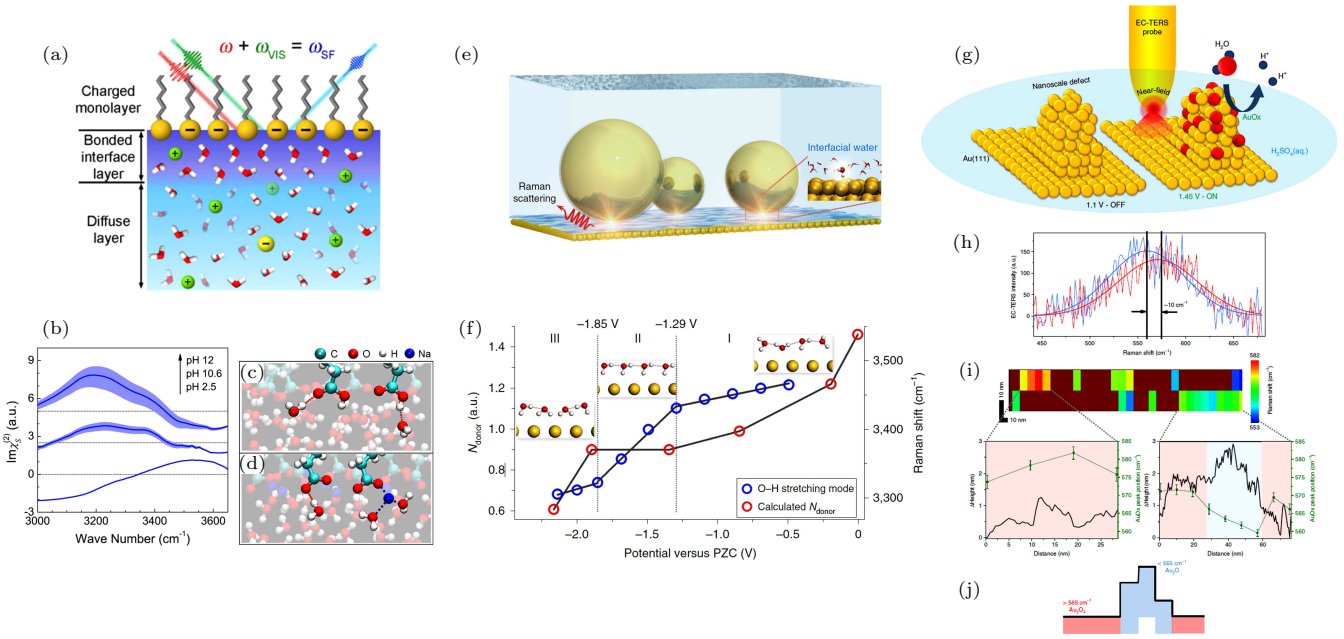


Fig. 4. (a) Illustration of two regions at the charged water interface. (b) OH stretching spectra of the BIL of the lignoceric acid monolayer-water interface at three different pH values. At pH = 2.5 (the neutral interface), a negative OH stretching band below 3350 cm^{-1} extending beyond 3000 cm^{-1} dominates, arising from down-pointing OH of water and COOH in the fatty acid headgroups. At pH = 12 (nearly fully deprotonated interface), a broad positive band from 3000 cm^{-1} to 3450 cm^{-1} dominates, resulting from up-pointing OH of water molecules donor bonded to O of COO^-. (c)–(d) Side-view snapshots of the MD trajectories for the neutral and fully deprotonated fatty acid–water interfaces, respectively. (e) Schematic illustration of *in situ* electrochemical shell-isolated nanoparticle-enhanced Raman spectroscopy (SHINERS). (f) Potential-dependent evolution of the hydrogen-bond network of interfacial water. (g) Schematic of the EC-TERS *operando* measurement. Oxidation OFF state: left, 1.1 V vs. Pd-H. Oxidation ON state: right, 1.45 V vs. Pd-H. (h) Two kinds of EC-TER spectra recorded at different AuO_x defect locations and fitted by Gaussian peaks. (i) EC-TERS map in the region of catalytic defects. (j) Schematic illustration of the difference in AuO_x peak position. Panels (a)–(d) reproduced with permission from Ref. [179], (e)–(f) reproduced with permission from Ref. [187], and (g)–(j) reproduced with permission from Ref. [195].

It is notable that the most challenging part of the SFG technique is the spectral interpretation from atomistic level, which may be complemented by theoretical simulations to some extent.[180,181] Along with molecular dynamics (MD) simulations, Kumar *et al.* provided atomistic understanding of the distinct line-shape broadening of the hydroxyl group vibration in various organic liquid in contact with sapphire.[28] Lyu *et al.* found that by increasing the alkaline concentration, an additional red-shifted O–H peak in SFG on quartz appeared and was attributed to the strong hydrogen bond of water molecules with the OH^- adsorbed on the surface. The detailed realignment of interfacial water was revealed by MD and DFT simulation.[182]

SERS is another technique widely applied to acquire vi-

brational information on the plasmonic interfaces. Different from SFG, the SERS was focused more on bulk samples due to the difficulty of suppressing interferences from the adjoining bulk phases[183] and the majority of interfacial studies were related to electrochemistry, self-assembled monolayers, and biological relevance,[184] offering little insight into atomic-level interfacial structure. Interfacial water also attracts a lot of attention in SERS studies, where the variation of frequency and intensity of O–H stretching band can be induced by electrode potential[185] and solvated ions.[186] Recently, by combining SERS and *ab initio* molecular dynamics study, the electrified water structures at Au single-crystal electrode surface were elucidated at molecular level by Li *et al.*, revealing a concomitant structural transition of water molecules from 'parallel' to 'one-H-down' and then to 'two-H-down' towards negative potential scanning (Figs. 4(e)–4(f)).[187] Moreover, Shin *et al.* uncovered molecular structure of water in the nanogaps within the silver nano-particulates by SERS, suggesting a denser ice-VII-like molecular structure even in ambient conditions.[188]

TERS takes the advantages of SPM and SERS, allowing chemical imaging with nanometer resolution.[189] The performance of TERS in liquid was introduced by Zenobi *et al.*[190] for the first time and Zeng *et al.*[191] demonstrated that the existence of water layer can actually improve the spectral stability. TERS has been used to monitor catalytic reactions at the liquid/solid interface as well.[192,193] It was demonstrated that the electronic and catalytic properties of a bimetallic surface can be mapped with 3-nm resolution in ambient condition.[194] Under *operando* conditions, Pfisterer *et al.* revealed that the chemical active site at the liquid/solid interface could be spatially resolved with a precision of 10 nm.[195] Moreover, they observed that Au_2O_3 and Au_2O species could form reversibly at defect-terrace and protrusion sites on the defect at the same time (Figs. 4(g)–4(j)). Although the spatial resolution of TERS imaging can be routinely obtained at tens of nanometers in liquid and is experiencing a rapid increase recently,[196–201] it is still challenging for TERS to achieve atomic-scale resolution up to now due to the drifting effect, optical distortion, the uncontrollable condition of the immersed tip, and the balance between the sharp tip able to acquire high resolution image and appropriate plasmonic properties to enhance the Raman signal. It is predictable that the TERS will become a powerful tool in the near future for investigating liquid/solid interfacial phenomena, including the detailed water structure.

3. Emerging techniques for characterization of liquid/solid interfaces

3.1. SPM combined with nitrogen-vacancy center technology (NV-SPM)

Although SPM can achieve atomic resolution, it inevitably induces perturbation to the liquid/solid interface by the excitation of the tunneling electrons or the tip–substrate interactions. For conventional spectroscopic methods, such as optical spectroscopy, neutron scattering, and nuclear magnetic resonance (NMR), they are almost non-invasive, but suffering from broadening and averaging effects due to the limitation of spatial resolution.

Nitrogen-vacancy (NV) center is an atomic defect in diamond, consisting of a substitutional nitrogen atom and an adjacent vacancy. Its spin states can be well manipulated by blue laser and microwaves and read out by red fluorescence. The resulting coherent spin evolution is very sensitive to the weak external signals, such as magnetic field, electric field, temperature, strain, and so on. Theoretically, the sensitivity of NV-center is extremely high, allowing the detection of the spin of a single proton and the electric field of a single elementary charge. In addition, the NV-center is buried inside the diamond (several nanometers below the surface), so it can work in the harshest environments such as acid/corrosive solutions, while still maintaining the excellent coherence. Most importantly, the interaction between the atomic NV-center and the targets is quite weak, corresponding to non-invasive sensing.

When employing NV-center as the scanning probe, the so-called NV-SPM can overcome many limitations in probing liquid/solid interface. In particular, it is worth mentioning that NV-SPM can conduct magnetic resonance imaging at nanoscale or even atomic scale. For example, the fluctuating external nuclear/electron spins in aqueous solution may lead to the enhancement of NV spin−lattice relaxation, which enables NV to image paramagnetic species and protons under physiological conditions.[202] What is more, the molecular dynamics at a solid–liquid interface can be also obtained by correlation signal from protons.[203,204] By applying A.C. electric field using the metal tip, it is possible to measure the frequency-dependent dielectric response of the interfacial water with nanometer resolution.

3.2. Multifunctional AFM techniques for battery characterization

AFM can be operated under realistic *operando* conditions to reveal detailed mechanism underlying electrochemical processes at liquid/solid interface, such as the interfacial evolution in batteries.[205–207] Establishing the relationship between microscopic structure and performance may help to promote next-generation batteries.[208,209] As a prototype, electrochemical AFM (EC-AFM) is the most widely used setup controlled by a potentiostat or galvanostat.[210–212] The application of EC-AFM ranges from the characterizations of morphology evolution on anodes (highly oriented pyrolytic graphite (HOPG),[213–217] graphite,[218,219] iron,[220] Li,[221] etc.) and cathodes (Li_xCoO_2,[222–224] $LiFePO_4$,[225] V_2O_5,[226] $LiMnPO_4$[227]) to the formation of

Li-dendrite.[221,228] Moreover, the onset[229,230] and dynamic process of solid electrolyte interface (SEI) formation[231–234] and morphological changes influenced by the types,[226,235,236] additives,[237–239] and concentration[240] of electrolyte salts or test temperature[241] were briefly studied at the nanoscale, indicating the inhomogeneous nature of SEI.[242]

Apart from EC-AFM, a great number of advanced AFM-based techniques have been applied for the studies of battery materials and interfaces, such as conductive AFM (C-AFM), electro-chemical strain microscope (ESM), and Kelvin probe force microscope (KPFM).[243] ESM developed by Kalinin[244–246] provides microscopic details of ionic or electronic transport process in battery under operation, via the localized measurements of volumetric strain induced by voltage pulse.[245,247,248] Another valid technique to gain fundamental understanding of interfacial electrical properties is KPFM,[249] which measures the surface potential between the sample and AFM tip. It can be applied to study the effects of surface charges on ionic intercalation[250] and the relationship between the distribution of lithium ions and the capacity decay.[251] Despite that AFM is a very powerful tool in the context of battery characterization at the nanoscale, it is still very challenging to obtain atomic-scale information. The development of low noise cantilever deflection sensor[105] and various drift-compensated data acquisition schemes[106,107] are promising to defeat this limitation in the near future.

3.3. *Ex-situ* SPM measurements under UHV condition

The approaches to study the solid–liquid interface mentioned above are all applied *in situ* under ambient condition. Because of the thermal noise, instability of tip, interferences by faradaic or capacitive currents, the achieved resolution is much poorer compared with that obtained under ultrahigh vacuum (UHV) conditions and low temperatures.

For the reason that most of liquid placed in UHV will be pumped away instantly, liquid/solid interfacial research should be carried out *ex situ* under UHV condition. This method is suitable for the systems where the interfacial interaction is strong enough. The usual way is to temporarily immerse the solid surface into aqueous solution[252] or dose a droplet by a pipet[253] and then transfer the sample into the UHV chamber for pumping away the bulk liquid on the surface, leaving the interfacial liquid layers. Self-assembled organic molecules on the surface prepared via the methods aforementioned have been widely investigated by SPM.[254–256] While the exposure of the sample to atmosphere is inevitable in this process, causing sample contamination somehow and bringing trouble to high-resolution characterization.[257]

Diebold's group designed a UHV-compatible apparatus to dose ultrapure liquid water on well-prepared and characterized substrate without air exposure.[258] This method can avoid sample contamination by ubiquitous environmental species, which shows high affinity to the sample surface. By taking advantage of this set-up, they clarified that exposing $TiO_2(110)$ surface to ultrapure H_2O in vacuum leading to (1×1) structure[259] rather than (2×1) structure claimed in others works,[252,253] where the latter was identified as the absorption of formic and acetic acids present in air. Such a method is also viable for water with other metal oxide surfaces, such as $Fe_3O_4(001)$[260] and α-$Fe_2O_3(1\bar{1}02)$.[261] *Ex-situ* measurements of liquid/solid interface under UHV can indeed provide atomic-scale insights into the interfacial processes, but the concern is that the few-liquid-layer left on the surface might be too far from the realistic liquid/solid condition.

3.4. Cryo-scanning transmission electron microscopy

Transmission electron microscopy (TEM) is rarely involved in earlier interfacial researches due to the reason that measurements should be operated under vacuum conditions and high-energy electrons not only bring perturbation to native environment at interface but also penetrate into the sample deeply such that the obtained information is not merely at liquid/solid interface. Those limitations can be overcome by vitrification,[262] which has been extensively use in the preparation of hydrated biological specimens. Fast freezing within milliseconds has proven to preserve the native state of interface and make the structural and chemical characterization possible in vacuum conditions. With the help of cryo-focused ion beam (cryo-FIB), it is possible to access the internal interfaces of thicker specimens.[263,264]

Recently, cryo-scanning transmission electron microscopy (cryo-STEM) was applied to analyze solid–liquid interfaces in lithium batteries, revealing detailed nanostructures such as dendrites at SEI with atomic resolution.[265,266] What is more, the fundamental role and influence of SEI nanostructures on battery performance can be clarified by monitoring the subtle morphological change as long with the number of cycling,[267] temperature variation,[268] and type of electrolyte.[269,270] It is predictable that cryo-STEM will become an important tool in the near future for investigating various liquid/solid interfaces beside the battery materials.

4. Summary

In conclusion, we have introduced and discussed various imaging and spectroscopic techniques aiming at understanding liquid/solid interface from an atomic-scale perspective. As a branch of SPM family, EC-STM provides a real-space imaging of the adsorbate–surface interaction under electrochemical condition, which sheds new light onto the microscopic picture underlying the macroscopic electrochemical phenomena. Representative advances include characterizing adsorption of

various anions as well as self-assembled molecules within the electrochemical double layer regime, atomic metal electrodeposition, metal corrosion and identification of catalytically active surface sites. NC-AFM enables high-resolution interfacial force measurements on insulating substrates, allowing for the investigation of the local water structure due to its sensitivity to the short-range force and water density. 3D-AFM can monitor distance-dependent behaviors of the interfacial interaction and image hydration layers both in lateral and vertical directions on different surfaces. Surface-sensitive vibrational spectroscopies including SFG, SERS, and TERS can extract both detailed chemical and structural information from the interface in a non-invasive manner. Atomic-scale understanding can be obtained with the help of theoretical calculations.

Furthermore, there are also emerging techniques for the atomic-scale characterization of liquid/solid interface. Firstly, non-perturbative NV-SPM might be a good candidate via locally probing the electron/nuclear spin of molecules in liquid with nanoscale precision, that is, nanoscale MRI. Secondly, we introduced multifunctional AFM-based techniques applied to address the interfacial phenomena in batteries under operation. Thirdly, *ex-situ* measurements of liquid/solid interface under UHV and cryogenic environment can reveal some basic aspects of liquid/solid interaction with unprecedented resolution. Lastly, the combination of fast-freezing technique and STEM enables the structural and chemical characterization of liquid/solid interface with atomic resolution, even for deep buried interface. It is reasonable to predict that the characterization of liquid/solid interface from atomic-scale perspective, especially the detailed solvent-solid interaction, will experience a rapid growth in the foreseeable future.

References

[1] Somorjai G A and Li Y 2010 *Introduction to surface chemistry and catalysis* (John Wiley & Sons)
[2] Wandelt K and Thurgate S 2002 *Solid-Liquid Interfaces: Macroscopic Phenomena—Microscopic Understanding*, Vol. 85 (Springer Science & Business Media)
[3] Baró A M and Reifenberger R G 2012 *Atomic force microscopy in liquid: biological applications* (John Wiley & Sons)
[4] Shchukarev A 2006 *Adv. Colloid Interface Science* **122** 149
[5] Saka H, Sasaki K, Tsukimoto S and Arai S 2005 *J. Mater. Res.* **20** 1629
[6] Klein K L, Anderson I M and de Jonge N 2011 *J. Microsc* **242** 117
[7] Shchukarev A and Ramstedt M 2017 *Surf. Interface Anal.* **49** 349
[8] Gewirth A A and Siegenthaler H 2013 *Nanoscale probes of the solid/liquid interface*, Vol. 288 (Springer Science & Business Media)
[9] Birdi K 2003 *Scanning probe microscopes: applications in science and technology* (CRC press)
[10] Guo J, Bian K, Lin Z and Jiang Y 2016 *J. Chem. Phys.* **145** 160901
[11] Herpich M, Friedl J and Stimming U 2015 *Surface Science Tools for Nanomaterials Characterization* (Springer) p. 1
[12] Gentz K and Wandelt K 2012 *Chimia (Aarau)* **66** 44
[13] Magnussen O M 2002 *Chem. Rev.* **102** 679
[14] Nowicki M and Wandelt K 2020 *Surf. Interface Sci.: Interfac. Electrochem.* **8** 517
[15] Liang Y, Pfisterer J H, McLaughlin D, Csoklich C, Seidl L, Bandarenka A S and Schneider O 2019 *Small Methods* **3** 1800387
[16] Böller B, Durner K M and Wintterlin J 2019 *Nat. Catal.* **2** 1027
[17] Yagati A K, Min J and Choi J W 2014 *Electrochemical Scanning Tunneling Microscopy (ECSTM)-From Theory to Future Applications*
[18] Niu L, Yin Y, Guo W, Lu M, Qin R and Chen S 2009 *J. Mater. Sci.* **44** 4511
[19] Budevski E B, Staikov G T and Lorenz W J 2008 *Electrochemical phase formation and growth: an introduction to the initial stages of metal deposition* (John Wiley & Sons)
[20] Oviedo O A, Reinaudi L, García S G and Leiva E P M 2016 *Underpotential Deposition* (Springer) p. 91
[21] Binnig G, Gerber C, Stoll E, Albrecht T and Quate C 1987 *Europhys. Lett.* **3** 1281
[22] Putnis A 2014 *Science* **343** 1441
[23] Verma A and Sharma A 2010 *Adv. Mater.* **22** 5306
[24] Dufrêne Y F, Ando T, Garcia R, Alsteens D, Martinez-Martin D, Engel A, Gerber C and Müller D 2017 *Nat. Nanotechnol.* **12** 295
[25] Maver U, Velnar T, Gaberšček M, Planinšek O and Finšgar M 2016 *Trends Anal. Chem.* **80** 96
[26] Fukuma T and Garcia R 2018 *ACS Nano* **12** 11785
[27] Miranda P B and Shen Y R 1999 *J. Phys. Chem. B* **103** 3292
[28] Kumar N, Kaur S, Kumar R, Wilson M C, Bekele S, Tsige M and Dhinojwala A 2019 *J. Phys. Chem. C* **123** 30447
[29] Zaera F 2012 *Chem. Rev.* **112** 2920
[30] Shi H, Lercher J A and Yu X Y 2015 *Catal. Sci. & Technol.* **5** 3035
[31] Zaera F 2014 *Chem. Soc. Rev.* **43** 7624
[32] Zhang B and Wang E 1994 *Electrochim. Acta* **39** 103
[33] Zhu L, Claude-Montigny B and Gattrell M 2005 *Appl. Surf. Sci.* **252** 1833
[34] Stojek Z 2010 *The electrical double layer and its structure* (Springer) p. 3
[35] Pham D T, Keller H, Breuer S, Huemann S, Hai N T N, Zoerlein C, Wandelt K and Broekmann P 2009 *CHIMIA Int. J. For Chem.* **63** 115
[36] Kim Y G, Baricuatro J H, Soriaga M P and Suggs D W 2001 *J. Electroanal. Chem.* **509** 170
[37] Goletti C, Bussetti G, Violante A, Bonanni B, Di Giovannantonio M, Serrano G, Breuer S, Gentz K and Wandelt K 2015 *J. Phys. Chem. C* **119** 1782
[38] Yamada T, Ogaki K, Okubo S and Itaya K 1996 *Surf. Sci.* **369** 321
[39] Zou S Z, Gao X P and Weaver M J 2000 *Surf. Sci.* **452** 44
[40] Schweizer M and Kolb D M 2003 *Surf. Sci.* **544** 93
[41] Cuesta A, Kleinert M and Kolb D M 2000 *PCCP* **2** 5684
[42] Spänig A, Broekmann P and Wandelt K 2005 *Electrochim. Acta* **50** 4289
[43] Spaenig A, Broekmann P and Wandelt K 2003 *Z. Phys. Chem.* **217** 459
[44] Safarowsky C, Spaenig A, Broekmann P and Wandelt K 2003 *Surf. Sci.* **538** 137
[45] Magnussen O M, Ocko B M, Wang J X and Adzic R R 1996 *J. Phys. Chem.* **100** 5500
[46] Andryushechkin B V, Zhidomirov G M, Eltsov K N, Hladchanka Y V and Korlyukov A A 2009 *Phys. Rev. B* **80** 125409
[47] Ye S, Ishibashi C and Uosaki K 1999 *Langmuir* **15** 807
[48] Polewska W, Vogt M R, Magnussen O M and Behm R J 1999 *J. Phys. Chem. B* **103** 10440
[49] Kim Y G, Kim J Y, Thambidurai C and Stickney J L 2007 *Langmuir* **23** 2539
[50] Hümann S, Hommrich J and Wandelt K 2003 *Thin Solid Films* **428** 76
[51] Madry B, Wandelt K and Nowicki M 2016 *Electrochim. Acta* **217** 249
[52] Yan J W, Wu J M, Wu Q, Xie Z X and Mao B W 2003 *Langmuir* **19** 7948
[53] Pao T, Chen Y, Chen S and Yau S 2013 *J. Phys. Chem. C* **117** 26659
[54] Hommrich J, Humann S and Wandelt K 2002 *Faraday Discuss.* **121** 129
[55] Wu Z L and Yau S L 2001 *Langmuir* **17** 4627
[56] Madry B, Wandelt K and Nowicki M 2015 *Surf. Sci.* **637-638** 77
[57] Li S S, Northrop B H, Yuan Q H, Wan L J and Stang P J 2009 *Acc. Chem. Res.* **42** 249
[58] De Feyter S, Miura A, Yao S, Chen Z, Wurthner F, Jonkheijm P, Schenning A P H J, Meijer E W and De Schryver F C 2005 *Nano Lett.* **5** 77
[59] Zhang X, Chen T, Chen Q, Wang L and Wan L J 2009 *Phys. Chem. Chem. Phys.* **11** 7708
[60] MacLeod J M, Lipton-Duffin J, Fu C, Taerum T, Perepichka D F and Rosei F 2017 *ACS Nano* **11** 8901
[61] Gutzler R, Fu C, Dadvand A, Hua Y, MacLeod J M, Rosei F and Perepichka D F 2012 *Nanoscale* **4** 5965

[62] Gutzler R, Ivasenko O, Fu C, Brusso J L, Rosei F and Perepichka D F 2011 *Chem. Commun. (Camb)* **47** 9453
[63] Silly F 2013 *J. Phys. Chem. C* **117** 20244
[64] Zheng Q N, Liu X H, Chen T, Yan H J, Cook T, Wang D, Stang P J and Wan L J 2015 *J. Am. Chem. Soc.* **137** 6128
[65] Bleger D, Kreher D, Mathevet F, Attias A J, Schull G, Huard A, Douillard L, Fiorini-Debuischert C and Charra F 2007 *Angew Chem. Int. Ed Engl* **46** 7404
[66] Xue Y and Zimmt M B 2011 *Chem. Commun. (Camb)* **47** 8832
[67] Xue Y and Zimmt M B 2012 *J. Am. Chem. Soc.* **134** 4513
[68] Bhattarai A, Mazur U and Hipps K W 2014 *J. Am. Chem. Soc.* **136** 2142
[69] Jahanbekam A, Vorpahl S, Mazur U and Hipps K W 2013 *J. Phys. Chem. C* **117** 2914
[70] Li Y, Liu C, Xie Y, Li X, Li X, Fan X, Deng K, Zeng Q and Wang C 2013 *Phys. Chem. Chem. Phys.* **15** 125
[71] Gatti R, MacLeod J M, Lipton-Duffin J A, Moiseev A G, Perepichka D F and Rosei F 2014 *J. Phys. Chem. C* **118** 25505
[72] Yang Y and Wang C 2009 *Curr. Opin. Colloid Interface Sci.* **14** 135
[73] De Feyter S and De Schryver F C 2005 *J. Phys. Chem. B* **109** 4290
[74] Otsuki J 2010 *Coord. Chem. Rev.* **254** 2311
[75] Cui D, MacLeod J M and Rosei F 2018 *Chem. Commun. (Camb)* **54** 10527
[76] Li J, Zu X, Qian Y, Duan W, Xiao X and Zeng Q 2020 *Chin. Chem. Lett.* **31** 10
[77] He Y, Ye T and Borguet E 2002 *J. Am. Chem. Soc.* **124** 11964
[78] Kunitake M, Akiba U, Batina N and Itaya K 1997 *Langmuir* **13** 1607
[79] Hai N T M, Gasparovic B, Wandelt K and Broekmann P 2007 *Surf. Sci.* **601** 2597
[80] Phan T H, Kosmala T and Wandelt K 2015 *Surf. Sci.* **631** 207
[81] Phan T H and Wandelt K 2013 *Surf. Sci.* **607** 82
[82] Hai N T, Furukawa S, Vosch T, De Feyter S, Broekmann P and Wandelt K 2009 *Phys. Chem. Chem. Phys.* **11** 5422
[83] Madry B, Morawski I, Kosmala T, Wandelt K and Nowicki M 2018 *Top. Catal.* **61** 1335
[84] Yoshimoto S, Higa N and Itaya K 2004 *J. Am. Chem. Soc.* **126** 8540
[85] Safarowsky C, Merz L, Rang A, Broekmann P, Hermann B A and Schalley C A 2004 *Angew Chem. Int. Ed Engl* **43** 1291
[86] Abrahami S T, Chiter F, Klein L H, Maurice V, Terryn H, Costa D and Marcus P 2019 *J. Phys. Chem. C* **123** 22228
[87] Schnur S and Groß A 2009 *New J. Phys.* **11** 125003
[88] Kim Y G, Soriaga J B, Vigh G and Soriaga M P 2000 *J. Colloid Interface Sci.* **227** 505
[89] Broekmann P, Wilms M, Spaenig A and Wandelt K 2001 *Prog. Surf. Sci.* **67** 59
[90] Jaramillo T F, Jorgensen K P, Bonde J, Nielsen J H, Horch S and Chorkendorff I 2007 *Science* **317** 100
[91] Zambelli T, Wintterlin J, Trost J and Ertl G 1996 *Science* **273** 1688
[92] Pfisterer J H K, Liang Y, Schneider O and Bandarenka A S 2017 *Nature* **549** 74
[93] Liang Y, McLaughlin D, Csoklich C, Schneider O and Bandarenka A S 2019 *Energy Environ. Sci.* **12** 351
[94] Liang Y, Csoklich C, McLaughlin D, Schneider O and Bandarenka A S 2019 *ACS Appl. Mater Interfaces* **11** 12476
[95] Wakisaka M, Asizawa S, Uchida H and Watanabe M 2010 *Phys. Chem. Chem. Phys.* **12** 4184
[96] Jacobse L, Huang Y F, Koper M T M and Rost M J 2018 *Nat. Mater.* **17** 277
[97] Jacobse L, Rost M J and Koper M T M 2019 *ACS Cent Sci.* **5** 1920
[98] Giessibl F J 2003 *Rev. Mod. Phys.* **75** 949
[99] Morita S, Giessibl F J, Meyer E and Wiesendanger R 2015 *Noncontact atomic force microscopy*, Vol. 3 (Springer)
[100] Gross L, Mohn F, Moll N, Liljeroth P and Meyer G 2009 *Science* **325** 1110
[101] Ma R, Cao D, Zhu C, Tian Y, Peng J, Guo J, Chen J, Li X Z, Francisco J S, Zeng X C, Xu L M, Wang E G and Jiang Y 2020 *Nature* **577** 60
[102] Peng J, Cao D, He Z, Guo J, Hapala P, Ma R, Cheng B, Chen J, Xie W J, Li X Z, Jelinek P, Xu L M, Gao Y Q, Wang E G and Jiang Y 2018 *Nature* **557** 701
[103] Albrecht T R, Grütter P, Horne D and Rugar D 1991 *J. Appl. Phys.* **69** 668
[104] Mokaberi B and Requicha A A G 2004 *IEEE International Conference on Robotics and Automation* **1–5** 416
[105] Fukuma T, Kimura M, Kobayashi K, Matsushige K and Yamada H 2005 *Rev. Sci. Instrum.* **76** 053704
[106] Abe M, Sugimoto Y, Namikawa T, Morita K, Oyabu N and Morita S 2007 *Appl. Phys. Lett.* **90** 203103
[107] Rahe P, Schutte J, Schniederberend W, Reichling M, Abe M, Sugimoto Y and Kuhnle A 2011 *Rev. Sci. Instrum.* **82** 063704
[108] Fukuma T, Kobayashi K, Matsushige K and Yamada H 2005 *Appl. Phys. Lett.* **87** 034101
[109] Kawasaki S, Holmström E, Takahashi R, Spijker P, Foster A S, Onishi H and Lippmaa M 2017 *J. Phys. Chem. C* **121** 2268
[110] Asakawa H, Holmström E, Foster A S, Kamimura S, Ohno T and Fukuma T 2018 *J. Phys. Chem. C* **122** 24085
[111] Imada H, Kimura K and Onishi H 2013 *Chem. Phys.* **419** 193
[112] Rode S, Oyabu N, Kobayashi K, Yamada H and Kuhnle A 2009 *Langmuir* **25** 2850
[113] Tracey J, Miyazawa K, Spijker P, Miyata K, Reischl B, Canova F F, Rohl A L, Fukuma T and Foster A S 2016 *Nanotechnology* **27** 415709
[114] Araki Y, Satoh H, Okumura M and Onishi H 2017 *Surf. Sci.* **665** 32
[115] Hiasa T, Sugihara T, Kimura K and Onishi H 2012 *J. Phys. Condens Matter* **24** 084011
[116] Suzuki K, Kitamura S-i, Tanaka S, Kobayashi K and Yamada H 2010 *Jpn. J. Appl. Phys.* **49** 08LB12
[117] Hiasa T, Kimura K and Onishi H 2012 *Colloids Surf. A* **396** 203
[118] Hiasa T, Kimura K and Onishi H 2012 *Phys. Chem. Chem. Phys.* **14** 8419
[119] Fukuma T, Higgins M J and Jarvis S P 2007 *Phys. Rev. Lett.* **98** 106101
[120] Sheikh K H, Giordani C, Kilpatrick J I and Jarvis S P 2011 *Langmuir* **27** 3749
[121] Yamada H, Kobayashi K, Fukuma T, Hirata Y, Kajita T and Matsushige K 2009 *Appl. Phys. Express* **2** 095007
[122] Kimura K, Ido S, Oyabu N, Kobayashi K, Hirata Y, Imai T and Yamada H 2010 *J. Chem. Phys.* **132** 194705
[123] Nagashima K, Abe M, Morita S, Oyabu N, Kobayashi K, Yamada H, Ohta M, Kokawa R, Murai R, Matsumura H, Adachi H, Takano K, Murakami S, Inoue T and Mori Y 2010 *J. Vac. Sci. Technol. B* **28** C4C11
[124] Kominami H, Kobayashi K, Ido S, Kimiya H and Yamada H 2018 *RSC Adv.* **8** 29378
[125] Kominami H, Kobayashi K and Yamada H 2019 *Sci. Rep.* **9** 6851
[126] Xue S, Sasahara A and Onishi H 2020 *J. Chem. Phys.* **152** 054703
[127] Miyata K, Tracey J, Miyazawa K, Haapasilta V, Spijker P, Kawagoe Y, Foster A S, Tsukamoto K and Fukuma T 2017 *Nano Lett.* **17** 4083
[128] Giessibl F J 2019 *Rev. Sci. Instrum.* **90** 011101
[129] Purckhauer K, Weymouth A J, Pfeffer K, Kullmann L, Mulvihill E, Krahn M P, Muller D J and Giessibl F J 2018 *Sci. Rep.* **8** 9330
[130] Ichii T, Negami M and Sugimura H 2014 *J. Phys. Chem. C* **118** 26803
[131] Mungse H P, Ichii T, Utsunomiya T and Sugimura H 2018 *MRS Adv.* **3** 2725
[132] Rodenbücher C, Wippermann K and Korte C 2019 *Appl. Sci.* **9** 2207
[133] Hölscher H, Langkat S M, Schwarz A and Wiesendanger R 2002 *Appl. Phys. Lett.* **81** 4428
[134] Marutschke C P 2015 *Three-Dimensional Imaging of the Solid-Liquid Interface with High-Resolution Atomic Force Microscopy* (Verlag nicht ermittelbar)
[135] Baykara M Z, Schwendemann T C, Altman E I and Schwarz U D 2010 *Adv. Mater.* **22** 2838
[136] Albers B J, Schwendemann T C, Baykara M Z, Pilet N, Liebmann M, Altman E I and Schwarz U D 2009 *Nanotechnology* **20** 264002
[137] Fukuma T, Higgins M J and Jarvis S P 2007 *Biophys. J.* **92** 3603
[138] Fukuma T 2010 *Sci. Technol. Adv. Mater.* **11** 033003
[139] Fukuma T, Ueda Y, Yoshioka S and Asakawa H 2010 *Phys. Rev. Lett.* **104** 016101
[140] Kobayashi K, Oyabu N, Kimura K, Ido S, Suzuki K, Imai T, Tagami K, Tsukada M and Yamada H 2013 *J. Chem. Phys.* **138** 184704
[141] Garcia R and Herruzo E T 2012 *Nat. Nanotechnol.* **7** 217
[142] Taranovskyy A, Tansel T and Magnussen O M 2010 *Phys. Rev. Lett.* **104** 106101
[143] Martin-Jimenez D, Chacon E, Tarazona P and Garcia R 2016 *Nat Commun.* **7** 12164
[144] Hollingsworth M D 2009 *Science* **326** 1194
[145] Dunne J P, Hales B and Toggweiler J R 2012 *Global Biogeochem. Cycles* **26** GB3023

[146] Marutschke C, Walters D, Walters D, Hermes I, Bechstein R and Kuhnle A 2014 *Nanotechnology* **25** 335703
[147] Pina C M, Pimentel C and García-Merino M 2010 *Surf. Sci.* **604** 1877
[148] Imada H, Kimura K and Onishi H 2013 *Langmuir* **29** 10744
[149] Reischl B, Raiteri P, Gale J D and Rohl A L 2019 *J. Phys. Chem. C* **123** 14985
[150] Fukuma T, Reischl B, Kobayashi N, Spijker P, Canova F F, Miyazawa K and Foster A S 2015 *Phys. Rev. B* **92** 155412
[151] Songen H, Marutschke C, Spijker P, Holmgren E, Hermes I, Bechstein R, Klassen S, Tracey J, Foster A S and Kuhnle A 2017 *Langmuir* **33** 125
[152] Hiasa T, Kimura K, Onishi H, Ohta M, Watanabe K, Kokawa R, Oyabu N, Kobayashi K and Yamada H 2010 *J. Phys. Chem. C* **114** 21423
[153] Suzuki K, Oyabu N, Kobayashi K, Matsushige K and Yamada H 2011 *Appl. Phys. Express* **4** 125102
[154] Suzuki K, Kobayashi K, Oyabu N, Matsushige K and Yamada H 2014 *J. Chem. Phys.* **140** 054704
[155] Nishioka R, Hiasa T, Kimura K and Onishi H 2013 *J. Phys. Chem. C* **117** 2939
[156] Asakawa H, Yoshioka S, Nishimura K-i and Fukuma T 2012 *ACS Nano* **6** 9013
[157] Hiasa T, Kimura K and Onishi H 2012 *J. Phys. Chem. C* **116** 26475
[158] Umeda K, Zivanovic L, Kobayashi K, Ritala J, Kominami H, Spijker P, Foster A S and Yamada H 2017 *Nat Commun.* **8** 2111
[159] Miranda P B and Shen Y R 1999 *J. Phys. Chem. B* **103** 3292
[160] Li X and Rupprechter G 2019 *Chin. J. Catal.* **40** 1655
[161] Hosseinpour S, Roeters S J, Bonn M, Peukert W, Woutersen S and Weidner T 2020 *Chem. Rev.* **120** 3420
[162] Chen X, Wang J, Sniadecki J J, Even M A and Chen Z 2005 *Langmuir* **21** 2662
[163] Mifflin A L, Velarde L, Ho J, Psciuk B T, Negre C F, Ebben C J, Upshur M A, Lu Z, Strick B L, Thomson R J, Batista V S, Wang H F and Geiger F M 2015 *J. Phys. Chem. A* **119** 1292
[164] Buchbinder A M, Weitz E and Geiger F M 2009 *J. Phys. Chem. C* **114** 554
[165] Liu W T and Shen Y R 2014 *Proc. Natl Acad. Sci. USA* **111** 1293
[166] Bozzini B, De Gaudenzi G P, Busson B, Humbert C, Six C, Gayral A and Tadjeddine A 2010 *J. Power Sources* **195** 4119
[167] Zhou W, Inoue S, Iwahashi T, Kanai K, Seki K, Miyamae T, Kim D, Katayama Y and Ouchi Y 2010 *Electrochem. Commun.* **12** 672
[168] Baldelli S, Bao J, Wu W and Pei S S 2011 *Chem. Phys. Lett.* **516** 171
[169] Du Q, Freysz E and Shen Y R 1994 *Phys. Rev. Lett.* **72** 238
[170] Yeganeh M, Dougal S and Pink H 1999 *Phys. Rev. Lett.* **83** 1179
[171] Jena K C and Hore D K 2010 *Phys. Chem. Chem. Phys.* **12** 14383
[172] Asay D B and Kim S H 2005 *J. Phys. Chem. B* **109** 16760
[173] Yang Z, Bertram A K and Chou K C 2011 *J. Phys. Chem. Lett.* **2** 1232
[174] Noguchi H, Okada T and Uosaki K 2008 *Electrochim. Acta* **53** 6841
[175] Yang Z, Li Q and Chou K C 2009 *J. Phys. Chem. C* **113** 8201
[176] Piontek S M, Tuladhar A, Marshall T and Borguet E 2019 *J. Phys. Chem. C* **123** 18315
[177] Covert P A, Jena K C and Hore D K 2014 *J. Phys. Chem. Lett.* **5** 143
[178] Jena K C, Covert P A and Hore D K 2011 *J. Phys. Chem. Lett.* **2** 1056
[179] Wen Y C, Zha S, Liu X, Yang S, Guo P, Shi G, Fang H, Shen Y R and Tian C 2016 *Phys. Rev. Lett.* **116** 016101
[180] Pfeiffer-Laplaud M and Gaigeot M P 2016 *J. Phys. Chem. C* **120** 4866
[181] Kroutil O, Chval Z, Skelton A A and Předota M 2015 *J. Phys. Chem. C* **119** 9274
[182] Lyu Y, Wang Y, Wang S, Liu B and Du H 2019 *Langmuir* **35** 11651
[183] Weaver M J, Zou S and Chan H Y 2000 *Anal. Chem.* **72** 38A
[184] Langer J, Jimenez de Aberasturi D, *et al.* 2020 *ACS Nano* **14** 28
[185] Chen Y, Zou S, Huang K and Tian Z 1998 *J. Raman Spectroscopy* **29** 749
[186] Zou S, Chen Y, Mao B, Ren B and Tian Z 1997 *J. Electroanal. Chem.* **424** 19
[187] Li C Y, Le J B, Wang Y H, Chen S, Yang Z L, Li J F, Cheng J and Tian Z Q 2019 *Nat. Mater.* **18** 697
[188] Shin D, Hwang J and Jhe W 2019 *Nat Commun.* **10** 286
[189] Wang X, Huang S C, Huang T X, Su H S, Zhong J H, Zeng Z C, Li M H and Ren B 2017 *Chem. Soc. Rev.* **46** 4020
[190] Schmid T, Yeo B S, Leong G, Stadler J and Zenobi R 2009 *J. Raman Spectrosc.* **40** 1392
[191] Zeng Z C, Huang S C, Wu D Y, Meng L Y, Li M H, Huang T X, Zhong J H, Wang X, Yang Z L and Ren B 2015 *J. Am. Chem. Soc.* **137** 11928
[192] van Schrojenstein Lantman E M, Deckert-Gaudig T, Mank A J, Deckert V and Weckhuysen B M 2012 *Nat. Nanotechnol.* **7** 583
[193] Kumar N, Stephanidis B, Zenobi R, Wain A J and Roy D 2015 *Nanoscale* **7** 7133
[194] Zhong J H, Jin X, Meng L, Wang X, Su H S, Yang Z L, Williams C T and Ren B 2017 *Nat. Nanotechnol.* **12** 132
[195] Pfisterer J H K, Baghernejad M, Giuzio G and Domke K F 2019 *Nat Commun.* **10** 5702
[196] Pienpinijtham P, Vantasin S, Kitahama Y, Ekgasit S and Ozaki Y 2016 *J. Phys. Chem. C* **120** 14663
[197] Martin Sabanes N, Driessen L M and Domke K F 2016 *Anal. Chem.* **88** 7108
[198] Touzalin T, Dauphin A L, Joiret S, Lucas I T and Maisonhaute E 2016 *Phys. Chem. Chem. Phys.* **18** 15510
[199] Bhattarai A, Joly A G, Krayev A and El-Khoury P Z 2019 *J. Phys. Chem. C* **123** 7376
[200] Jiang S, Chen Z, Chen X, Nguyen D, Mattei M, Goubert G and Van Duyne R P 2019 *J. Phys. Chem. C* **123** 9852
[201] Bhattarai A and El-Khoury P Z 2019 *J. Phys. Chem. Lett.* **10** 2817
[202] Ziem F C, Gotz N S, Zappe A, Steinert S and Wrachtrup J 2013 *Nano Lett.* **13** 4093
[203] Staudacher T, Raatz N, Pezzagna S, Meijer J, Reinhard F, Meriles C A and Wrachtrup J 2015 *Nat Commun.* **6** 8527
[204] Shagieva F, Zaiser S, Neumann P, Dasari D B R, Stohr R, Denisenko A, Reuter R, Meriles C A and Wrachtrup J 2018 *Nano Lett.* **18** 3731
[205] Kempaiah R, Vasudevamurthy G and Subramanian A 2019 *Nano Energy* **65** 103925
[206] Tripathi A M, Su W N and Hwang B J 2018 *Chem. Soc. Rev.* **47** 736
[207] Wang S, Liu Q, Zhao C, Lv F, Qin X, Du H, Kang F and Li B 2018 *Energy & Environ. Mater.* **1** 28
[208] Goodenough J B 2014 *Energy Environ. Sci.* **7** 14
[209] Park M, Ryu J, Wang W and Cho J 2017 *Nat. Rev. Mater.* **2** 16080
[210] Aurbach D 1996 *J. Electrochem. Soc.* **143** 3525
[211] Aurbach D and Cohen Y 1999 *Electrochem. Solid State Lett.* **2** 16
[212] Inaba M, Jeong S K and Ogumi Z 2011 *Electrochem. Soc. Interface* **20** 55
[213] Alliata D, Kotz R, Haas O and Siegenthaler H 1999 *Langmuir* **15** 8483
[214] Campana F P, Kötz R, Vetter J, Novák P and Siegenthaler H 2005 *Electrochem. Commun.* **7** 107
[215] Campana F P, Buqa H, Novák P, Kötz R and Siegenthaler H 2008 *Electrochem. Commun.* **10** 1590
[216] Jeong S K, Inaba M, Mogi R, Iriyama Y, Abe T and Ogumi Z 2001 *Langmuir* **17** 8281
[217] Jeong S K, Inaba M, Iriyama Y, Abe T and Ogumi Z 2003 *J. Power Sources* **119-121** 555
[218] Koltypin M, Cohen Y S, Markovsky B, Cohen Y and Aurbach D 2002 *Electrochem. Commun.* **4** 17
[219] Aurbach D, Koltypin M and Teller H 2002 *Langmuir* **18** 9000
[220] Weinrich H, Come J, Tempel H, Kungl H, Eichel R A and Balke N 2017 *Nano Energy* **41** 706
[221] Cohen Y S, Cohen Y and Aurbach D 2000 *J. Phys. Chem. B* **104** 12282
[222] Clémençon A, Appapillai A T, Kumar S and Shao-Horn Y 2007 *Electrochim. Acta* **52** 4572
[223] Park J, Kalnaus S, Han S, Lee Y K, Less G B, Dudney N J, Daniel C and Sastry A M 2013 *J. Power Sources* **222** 417
[224] Wu J, Yang S, Cai W, Bi Z, Shang G and Yao J 2017 *Sci. Rep.* **7** 11164
[225] Wu J, Cai W and Shang G 2016 *Nanoscale Res. Lett.* **11** 223
[226] Cohen Y S and Aurbach D 2004 *Electrochem. Commun.* **6** 536
[227] Doi T, Inaba M, Tsuchiya H, Jeong S K, Iriyama Y, Abe T and Ogumi Z 2008 *J. Power Sources* **180** 539
[228] Shen C, Hu G, Cheong L Z, Huang S, Zhang J G and Wang D 2018 *Small Methods* **2** 1700298
[229] Yoon I, Abraham D P, Lucht B L, Bower A F and Guduru P R 2016 *Adv. Energy Mater.* **6** 1600099
[230] Lacey S D, Wan J, von Wald Cresce A, Russell S M, Dai J, Bao W, Xu K and Hu L 2015 *Nano Lett.* **15** 1018
[231] Novak P, Joho F, Lanz M, Rykart B, Panitz J C, Alliata D, Kotz R and Haas O 2001 *J. Power Sources* **97-8** 39
[232] Tokranov A, Sheldon B W, Li C, Minne S and Xiao X 2014 *ACS Appl. Mater Interfaces* **6** 6672

[233] Domi Y, Ochida M, Tsubouchi S, Nakagawa H, Yamanaka T, Doi T, Abe T and Ogumi Z 2011 *J. Phys. Chem. C* **115** 25484
[234] Liu T, Lin L, Bi X, Tian L, Yang K, Liu J, Li M, Chen Z, Lu J, Amine K, Xu K and Pan F 2019 *Nat. Nanotechnol.* **14** 50
[235] Shi Y, Yan H J, Wen R and Wan L J 2017 *ACS Appl. Mater Interfaces* **9** 22063
[236] Shen C, Wang S, Jin Y and Han W Q 2015 *ACS Appl. Mater Interfaces* **7** 25441
[237] Lin L, Yang K, Tan R, Li M, Fu S, Liu T, Chen H and Pan F 2017 *J. Mater. Chem. A* **5** 19364
[238] v Cresce A, Russell S M, Baker D R, Gaskell K J and Xu K 2014 *Nano Lett.* **14** 1405
[239] Wang S, Yang K, Gao F, Wang D and Shen C 2016 *RSC Adv.* **6** 77105
[240] Liu X R, Wang L, Wan L J and Wang D 2015 *ACS Appl. Mater Interfaces* **7** 9573
[241] Edstrom K and Herranen M 2000 *J. Electrochem. Soc.* **147** 3628
[242] Zhang J, Wang R, Yang X, Lu W, Wu X, Wang X, Li H and Chen L 2012 *Nano Lett.* **12** 2153
[243] Chen X, Lai J, Shen Y, Chen Q and Chen L 2018 *Adv. Mater.* **30** 1802490
[244] Morozovska A N, Eliseev E A, Balke N and Kalinin S V 2010 *J. Appl. Phys.* **108** 053712
[245] Jesse S, Balke N, Eliseev E, Tselev A, Dudney N J, Morozovska A N and Kalinin S V 2011 *ACS Nano* **5** 9682
[246] Balke N, Jesse S, Kim Y, Adamczyk L, Tselev A, Ivanov I N, Dudney N J and Kalinin S V 2010 *Nano Lett.* **10** 3420
[247] Balke N, Jesse S, Morozovska A N, Eliseev E, Chung D W, Kim Y, Adamczyk L, Garcia R E, Dudney N and Kalinin S V 2010 *Nat. Nanotechnol.* **5** 749
[248] Yang S, Yan B, Li T, Zhu J, Lu L and Zeng K 2015 *Phys. Chem. Chem. Phys.* **17** 22235
[249] Nonnenmacher M, O'Boyle M P and Wickramasinghe H K 1991 *Appl. Phys. Lett.* **58** 2921
[250] Zhu J, Zeng K and Lu L 2012 *J. Appl. Phys.* **111** 063723
[251] Luchkin S Y, Amanieu H Y, Rosato D and Kholkin A L 2014 *J. Power Sources* **268** 887
[252] Hussain H, Tocci G, Woolcot T, Torrelles X, Pang C L, Humphrey D S, Yim C M, Grinter D C, Cabailh G, Bikondoa O, Lindsay R, Zegenhagen J, Michaelides A and Thornton G 2017 *Nat. Mater.* **16** 461
[253] Balajka J, Aschauer U, Mertens S F L, Selloni A, Schmid M and Diebold U 2017 *J. Phys. Chem. C Nanomater Interfaces* **121** 26424
[254] Newkome G R, Wang P, Moorefield C N, Cho T J, Mohapatra P P, Li S, Hwang S H, Lukoyanova O, Echegoyen L, Palagallo J A, Iancu V and Hla S W 2006 *Science* **312** 1782
[255] Song B, Kandapal S, Gu J, Zhang K, Reese A, Ying Y, Wang L, Wang H, Li Y, Wang M, Lu S, Hao X Q, Li X, Xu B and Li X 2018 *Nat Commun.* **9** 4575
[256] Zhang Z, Li Y, Song B, Zhang Y, Jiang X, Wang M, Trumbleson R, Liu C, Wang P, Hao X Q, Rojas T, Ngo A T, Sessler J L, Newkome G R, Hla S W and Li X 2020 *Nat Chem.* **12** 468
[257] Song A, Skibinski E S, DeBenedetti W J I, Ortoll-Bloch A G and Hines M A 2016 *J. Phys. Chem. C* **120** 9326
[258] Balajka J, Pavelec J, Komora M, Schmid M and Diebold U 2018 *Rev. Sci. Instrum.* **89** 083906
[259] Balajka J, Hines M A, DeBenedetti W J I, Komora M, Pavelec J, Schmid M and Diebold U 2018 *Science* **361** 786
[260] Kraushofer F, Mirabella F, Xu J, Pavelec J, Balajka J, Mullner M, Resch N, Jakub Z, Hulva J, Meier M, Schmid M, Diebold U and Parkinson G S 2019 *J. Chem. Phys.* **151** 154702
[261] Jakub Z, Kraushofer F, Bichler M, Balajka J, Hulva J, Pavelec J, Sokolović I, Müllner M, Setvin M, Schmid M, Diebold U, Blaha P and Parkinson G S 2019 *ACS Energy Lett.* **4** 390
[262] Dubochet J, Adrian M, Chang J J, Homo J C, Lepault J, McDowall A W and Schultz P 1988 *Q. Rev. Biophys.* **21** 129
[263] Zachman M J, Asenath-Smith E, Estroff L A and Kourkoutis L F 2016 *Microsc. Microanal.* **22** 1338
[264] Zachman M J, de Jonge N, Fischer R, Jungjohann K L and Perea D E 2019 *MRS Bull.* **44** 949
[265] Zachman M J, Tu Z, Choudhury S, Archer L A and Kourkoutis L F 2018 *Nature* **560** 345
[266] Li Y, Li Y, Pei A, Yan K, Sun Y, Wu C L, Joubert L M, Chin R, Koh A L, Yu Y, Perrino J, Butz B, Chu S and Cui Y 2017 *Science* **358** 506
[267] Huang W, Attia P M, Wang H, Renfrew S E, Jin N, Das S, Zhang Z, Boyle D T, Li Y, Bazant M Z, McCloskey B D, Chueh W C and Cui Y 2019 *Nano Lett.* **19** 5140
[268] Wang J, Huang W, Pei A, Li Y, Shi F, Yu X and Cui Y 2019 *Nat. Energy* **4** 664
[269] Li Y, Huang W, Li Y, Pei A, Boyle D T and Cui Y 2018 *Joule* **2** 2167
[270] Xu Y, Wu H, He Y, Chen Q, Zhang J G, Xu W and Wang C 2020 *Nano Lett.* **20** 418